LARGE SCALE CFD MODELLING OF WAVE PROPAGATION IN SULAFJORD FOR THE E39 PROJECT

Weizhi Wang[*], Hans Bihs[†], Arun Kamath[†],and Øivind Asgeir Arntsen[†]

Department of Civil and Environmental Engineering, Norwegian University of Science and Technology (NTNU), 7491 Trondheim, Norway

Abstract

The coastal high way project E39 aims at building a continuous ferry-free road connection along the west coast of Norway. One of the major challenges in the project is to replace ferries with new fjord-crossing methods such as floating bridges and floating tunnels. The unique topographies of the Norwegian fjords pose deep water conditions and large scale wave transformations. This makes it more complicated to analyse the wave loads on the floating structures. In order to have a better knowledge of the wave height distribution, wave direction and wave transformation details, accurate simulations of wave propagations with good representations of the free surfaces are demanded. CFD (Computational Fluid Dynamics) is able to capture most complexities of the wave physics with few assumptions and has been widely and successfully applied on hydrodynamics. With increasing computational capacities, it is possible to use CFD on large scale simulations. Therefore, large scale three dimensional simulations of wave propagations into Sulafjord are performed in this paper with the CFD model REEF3D. The spectra wave model SWAN is used to obtain the wave data from offshore data and give inputs for the CFD simulation. The CFD simulations are performed with both regular and irregular waves and give the details of the free surfaces and wave transformations in the fjord, the results of which are also compared with the wave model SWAN. REEF3D solves the incompressible Navier-Stokes equations with finite difference method and uses level-set method to capture the free surface under the two phase flow approximation. Together with the implements of high order schemes, REEF3D demonstrates high performance on wave hydrodynamics. The large scale Sulafjord simulation shows high resolution results and the details of wave transformations are well visualised. The results at wave probes are also compared between REEF3D and SWAN

Keywords: Large scale; CFD; Two phase flow; Level-set method; REEF3D; SWAN

---

[*]Corresponding author, weizhi.wang@ntnu.no

1   INTRODUCTION

The coastal highway project E39 is a major marine civil engineering project in Norway. As part of the National Transport Plan (NTP) for 2014-2023, it is aimed to build a continuous ferry-free road connection between Kristiansand and Trondheim along the west coast of Norway, which covers around 1100 km in distance with seven major fjord crossings according to Ellevset (2012). Three major bridge designs are proposed for fjord crossings, a single span suspension bridge, a floating bridge and a submerged tunnel summarised by Ellevset (2012). The floating structure designs put new demands for accurate wave propagation simulation into the fjords. The Norwegian fjords are very unique as most of them have very steep slopes with rather deep water conditions. For example, Hasselø (2015) points out that the research object Sulafjord is 3200m to 5000m wide and up to 450m deep. Though it is not the widest or deepest fjord, it has been chosen as the study case in this paper due to its representative features and reasonable domain size with respect to computation load. Besides, the study will make the numerical simulation keep pace with the ongoing field measurements in Sulafjord.

The numerical models for coastal simulation were initially developed with a statistical method based on significant wave height. But Thomas and Dwarakish (2015) points out that the requirement of a fine mesh in the coastal region due to the complex bathymetry demands the third generation wave models, such as MIKE 21 SW. Another third generation model is the spectral wave model Simulating Waves Near shore (SWAN) developed by Delft University of Technology and described by Thomas and Dwarakish (2015). Both MIKE 21 SW and SWAN give good results in terms of predicting energy spectrum and significant wave height. However, as they are phase-averaged wave models, Thomas and Dwarakish (2015) also points out that some phenomena like wave diffraction can not be represented well. Therefore, a high resolution phase-resolved numerical model is needed to reflect detailed wave phenomena in the fjords.

Another application in coastal and harbour engineering is a Boussinesq equation based wave model. Boussinesq type equations have been used successfully for shallow water simulations. Madsen and Srensen (1992) proposed improved versions of the Boussinesq equations which further reduce the limitation of its application due to water depth (d) and wave length (L), making it possible to simulate waves with d/L ratio of 0.6. But in Sulafjord, the d/L ratio can be greater than 1 which corresponds to deep water conditions, where Boussinesq equations are not applicable.

As Computational Fluid Dynamics (CFD) is able to capture most of the complexity in the flow field with few assumptions, it is becoming the new alternative for modelling in coastal engineering. However, the limitation of CFD application to coastal engineering is the high demand on the computational resources. In recent years, super computer infrastructure and parallel computation technology have been improved at a fast pace. With increasing computational resources and improved CFD tools, large domain simulations of wave propagation for Sulajord is possible with CFD. To meet this challenge, REEF3D has been developed by Bihs et al. (2016) at NTNU as a CFD code with focus on wave hydrodynamics by solving the incompressible Navier-Stokes equations and has been applied to a wide range of marine applications, for example, Alagan Chella et al. (2017) used the model for analysing the breaking

wave kinematics , Kamath et al. (2016) used the model for breaking wave-structure interaction and Bihs and Kamath (2016) simulated the floating body dynamics in waves with REEF3D. This paper presents the large scale CFD wave modelling at Sulafjord using REEF3D.

A simulation is firstly performed with the spectral wave model SWAN to approximate the wave properties at the fjord entrance from the offshore wave data. Three wave height probes are used in the SWAN model which correspond to the three locations of the field measurements. The resulting wave height and period at the probe at the fjord entrance are then used as inputs in the CFD simulation. A CFD simulation with a unidirectional regular wave and a CFD simulation with a unidirectional irregular wave are conducted using REEF3D. Wave height probes corresponding to the same locations as those in SWAN are also used in the CFD simulations. The resulting wave properties from all three numerical simulations are compared at wave probes and the phase-resolved results from the CFD simulations are visualised and analysed against the wave transformation physics.

2   NUMERICAL MODEL

2.1   Governing Equations

Water wave hydrodynamics comply with the mass conservation and momentum conservation, which are represented by the incompressible Navier-Stokes equations, as shown in Eqn. (1) and Eqn. (2). For large scale water waves, the turbulence effect is ignored, and thus the turbulence terms in the equations are excluded.

$$\frac{\partial u_i}{\partial x_i} = 0 \tag{1}$$

$$\frac{\partial u_i}{\partial t} + u_j \frac{\partial u_i}{\partial x_j} = -\frac{1}{\rho}\frac{\partial p}{\partial x_i} + \frac{\partial}{\partial x_j}\left[\nu\left(\frac{\partial u_i}{\partial x_j} + \frac{\partial u_j}{\partial x_i}\right)\right] + g_i \tag{2}$$

where u is the velocity, ρ is the fluid density, p is the pressure, ν is the kinematic viscosity and g the acceleration due to gravity.

REEF3D solves the governing equations on a structured Cartesian grid and is able to implement high-order schemes with finite difference method .

For the convection terms in the Navier-Stokes equations, the conservative fifth-order weighted essentially non-oscillatory (WENO) scheme is applied. According to Guang-Shan and Chi-Wang (1996), by using a convex combination of all stencils with each of them assigned with a weight, WENO is less sensitive to round-off errors and also has better smoothness of the flux.

The third-order Total-Variation-Diminishing (TVD) Runge-Kutta scheme proposed by Chi-Wang and Stanley (1988) is employed for time treatment in the momentum equations and the level set equations. The adaptive time step is also adopted in order to fulfil the

Courant-Friedrichs-Lewy(CFL) criterion as described by Griebel et al. (1998).

The Poisson equation for pressure is solved using the library of HYPRE (2016). The HYPRE library provides high performance solvers that make large and detailed simulations possible and solve the problems faster at large scales. With the HYPRE library, REEF3D is able to use BiCGStab proposed by Van Der Vorst (1992) as the iterative solver and geometric multi-grid PFMG developed by Falgout et al. (2006) as the pre-conditioner for the Poisson equations. As a result, the solver scales very well.

2.2   Numerical Wave Tank

The level set method is adopted to capture the free surface. Osher and Sethian (1988) descibes the level set function $\phi(\vec{x}, t)$ as a signed distance function which is designed so that it equals to zero at the interface and shows opposite signs in the two different phases, as shown in Eqn. (3).

$$\phi(\vec{x}, t) \begin{cases} > 0 \ if \ \vec{x} \in phase \ 1 \\ = 0 \ if \ \vec{x} \in \Gamma \\ < 0 \ if \ \vec{x} \in phase \ 2 \end{cases} \tag{3}$$

REEF3D is able to apply various wave theories, such as linear wave theory, $2nd$-order and $5th$-order Stokes waves and irregular wave theories. The equations to describe the waves include the velocities in the horizontal and vertical direction u and w and the level set function ϕ for the surface elevation. As an example, the equations for deep water linear wave theory are represented in Eqn. (4).

$$u(x, z, t)_{analytical} = \frac{\pi H}{T} \frac{cosh \left[k \left(z + d \right) \right]}{sinh \left(kd \right)} cos\theta$$
$$w(x, z, t)_{analytical} = \frac{\pi H}{T} \frac{sinh \left[k \left(z + d \right) \right]}{sinh \left(kd \right)} sin\theta \tag{4}$$
$$\phi(x, z, t)_{analytical} = \frac{H}{2} cos\theta - z + d$$

The wave phase θ and the wave number k are described in Eqn. (5):

$$k = \frac{2\pi}{L}$$
$$\theta = kx - \omega t \tag{5}$$

where H is the wave height, L is the wavelength, T is the wave period, ω is the angular wave frequency and z is the vertical coordinate measured from the still water level $z = 0$.

The wave is generated and absorbed using relaxation method proposed by Mayer et al. (1998). The relaxation function formulated by Jacobsen et al. (2012) is implemented as shown in Eqn. (6).

$$\Gamma(\widetilde{x}) = 1 - \frac{e^{(\widetilde{x}^{3.5})} - 1}{e - 1} \ for \ \widetilde{x} \in [0; 1] \tag{6}$$

where $\widetilde{x}$ is scaled to the length of the relaxation zone.

The velocities and the free surface level defined in Eqn. (4) together with the pressure are ramped up in the wave generation zone to the analytical values from the desired wave theory and the waves are released into the working zone in the tank. In the numerical beach, the velocities are reduced smoothly to zero, free surface is damped to still water level and the pressure is relaxed to hydrostatic pressure. The process is shown in Eqn. (7)

$$
\begin{aligned}
u(\widetilde{x})_{relaxed} &= \Gamma(\widetilde{x})u_{analytical} + (1 - \Gamma(\widetilde{x}))u_{computational} \\
w(\widetilde{x})_{relaxed} &= \Gamma(\widetilde{x})w_{analytical} + (1 - \Gamma(\widetilde{x}))w_{computational} \\
p(\widetilde{x})_{relaxed} &= \Gamma(\widetilde{x})p_{analytical} + (1 - \Gamma(\widetilde{x}))p_{computational} \\
\phi(\widetilde{x})_{relaxed} &= \Gamma(\widetilde{x})\phi_{analytical} + (1 - \Gamma(\widetilde{x}))\phi_{computational}
\end{aligned}
\tag{7}
$$

The complicated bathymetry of coastal region consisting of a set of scattered points is implemented using the inverse distance weighting method proposed by Shepard (1968). This method obtains the values at the unknown points by interpolating the weighted average of the values at the known scattered points. Additionally, an improved level set method is used for the geometric representation of the irregular solid boundary. As a result, the water surface is better captured near the irregular shoreline with very shallow water condition.

The irregular solid geometry at the seabed also poses a challenge to the boundary conditions. This challenge is solved by the ghost cell immersed boundary method (GCIBM) as described by Berthelsen and Faltinsen (2008). GCIBM makes the solution across the boundaries continuous by extrapolating data into the fictitious ghost cell. And therefore, the numerical discretisation deals with boundary conditions implicitly. The algorithm is originally based on the local directional approach in two dimensions developed by Berthelsen and Faltinsen (2008).

3 SULAFJORD SIMULATION

3.1 Sulafjord description

The bathymetry for Sulafjord is obtained from the Norwegian Mapping Authority Kartverket. Fig. 1 (a) provided by shows the geographical domain of the entire Sulafjord region. The preliminary designs of the fjord crossing and the crossing locations are shown in Fig.1(b) from Statensvegvesen (2015). Therefore, the main focus of the simulation is shown as a black box in Fig. 1. Norgeskart (2017) gives the most dangerous wave direction for the fjord as shown in Fig. 2 . In this paper, only unidirectional waves are simulated with the direction of the most dangerous waves. The ongoing field measurements are conducted at location D, A and B, as shown in Fig.1(a), the coordinates of the three probes in UTM 33 coordinate system are listed in Table 1. Values at probe I from SWAN are used as inputs in REEF3D, the coordinate of which is also shown in Table 1.

3.2 Swan simulation of Sulafjord and corresponding offshore area

Before the waves reach Sulafjord, large scale wave shoaling occurs, which have significant effect on wave properties. Therefore, in order to have reasonable wave inputs in the fjord
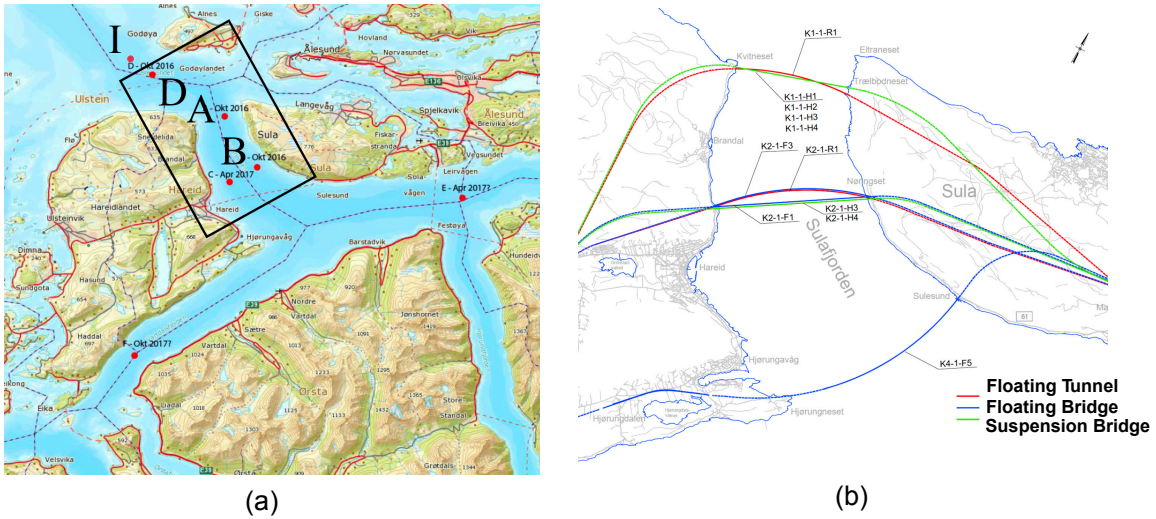
Figure 1: (a)Locations of the wave height probes in the Sulafjord measurements and the domain of focus shown as the black box, (b)possible fjord crossing locations

Table 1: The wave height probes at Sulafjord

Probe denotation	x coordinate	y coordinate
I	31600.00	6957000.00
D	33109.42	6956082.14
A	38596.05	6953729.83
B	40026.88	6950883.83

simulation, a spectral wave model simulation is used to get the wave properties from the offshore wave data. The initial wave properties are taken from offshore data according to the suggestion of the NORSOK (2007). The selected significant wave height is 16m, the period is 18s. The directional width of the directional spreading function is chosen to be 2. The bottom geometry is obtained from the Norwegian Mapping Authority Kartverket. To optimise the computational resources and accuracy, a nesting technic is applied. By nesting, the overall region is simulated with a coarse resolution; this simulation provides boundary values to a finer grid of smaller area, which again provides boundary input values to an even finer grid at an even smaller domain. Generally SWAN (2006) advises to reduce step size from one nesting level to the next by a factor of 2 or 3. The mean wave direction is chosen to be 315° so the waves in general agree with the most dangerous wave direction. The mesh convergence study is shown in Fig.4. Therefore, four nesting layers are used with the mesh size of 200m, 100m, 50m and 25m. The bottom geometry and the layers of nesting are demonstrated in Fig. 3, the resulting significant wave height distribution is shown in Fig. 5. The significant wave height at inlet probe I is 5.34m and the peak period is 16.86s, which is later used as input in the CFD simulations.
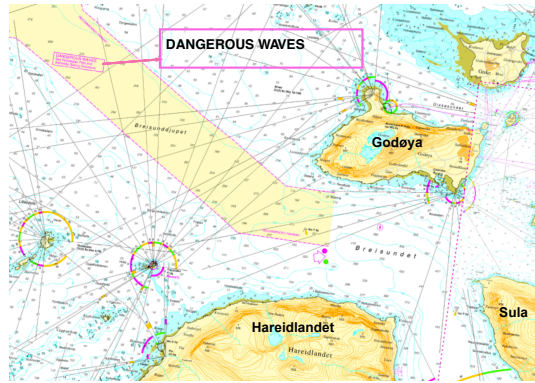
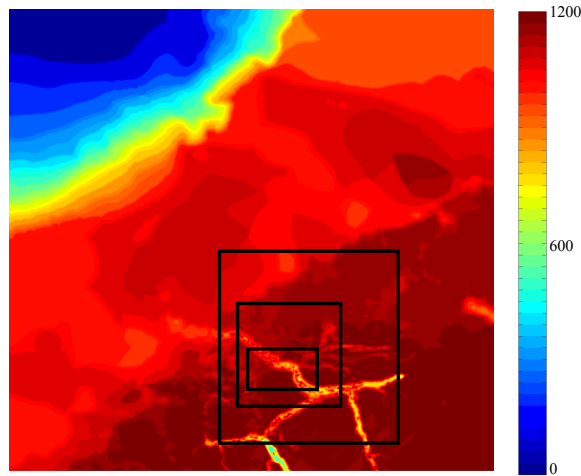Figure 2: Dangerous wave direction for Sulafjord

Figure 3: The bottom geometry of the SWAN simulation and the nesting layers in the simulation, the three black boxes represent the three nesting layers, smaller box has finer mesh

3.3 Wave tank set up of the CFD simulations

In order to focus on the fjord crossing region and align the numerical wave propagation direction with the most dangerous wave direction, the sub-sea topography is further extracted for a smaller domain, shown as a black box in Fig. 1. The geometry is then rotated anti-clockwise of $55°$ so that the wave can propagate from the left side of the wave tank. The final geometry used in the simulation is shown in Fig. 6. The corresponding numerical tank is 10000 m long and 9000 m wide and the maximum water depth is 447 m. The wave generation zone is shown as a black box and the numerical beaches are shown as yellow boxes in Fig. 6. Considering the computational resources, the mesh size is chosen to be 20 m. As the main focus is to demonstrate the feasibility of large scale simulation, and the large scale simulation is very time consuming, no further mesh convergence study is conducted at the current stage.

The results at probe I from the SWAN simulation are used directly in the CFD simula-
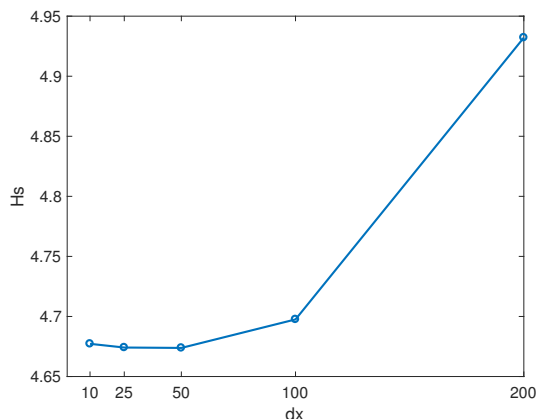
Figure 4: The mesh convergence study of the swan simulation

tions. The irregular wave consists of 700 wave components and the standard JONSWAP wave spectrum is used. The regular wave is a Stokes $5^t h$ wave of 5.34m wave height and 16.86s wave period.

3.4 CFD simulation results

The simulation results for both regular waves and irregular waves are shown in Fig. 7. Refraction can be observed along the fjord, where the wave propagation direction tends to be perpendicular to the bank at the near-shore area. The overlapping patterns of the refracted waves, diffracted waves and reflected waves can be seen around the tip of Sula island. The wave propagation is rather steady inside the fjord, with minor reflection from the banks. The different wave transformation phenomena are well presented in the simulation result. This gives CFD simulation a prominent advantage in comparison to the phase-averaged models where only the significant wave height contours are presented. From the fjord crossing infrastructure design point of view, the simulation is not only able to give the magnitudes of wave heights, but also the direction of the waves at specific locations and the interaction of different waves, which facilitate the analysis of wave loads.

The significant wave heights obtained from the SWAN simulation and the irregular wave simulation are compared with the mean wave heights from the regular wave simulation in Table 2. The mean wave periods are also compared. As can be seen, the regular wave simulation gives much higher wave height, indicating that the regular wave simulation with one propagation direction is too conservative from engineering point of view. The irregular wave CFD simulation also gives higher H_s than SWAN, but it is not easy to make a judgement of the accuracies. As SWAN is not performing well with the diffraction phenomenon as mentioned before by Thomas and Dwarakish (2015), the results at the probes inside the fjord are not considered to be very convincing. Meanwhile, the irregular wave CFD simulation does not account for the directional spreading function, which also leads to more conservative results. The data from the field measurements is only available for two months , which is not suitable for validation purpose. An observation of longer time is needed.
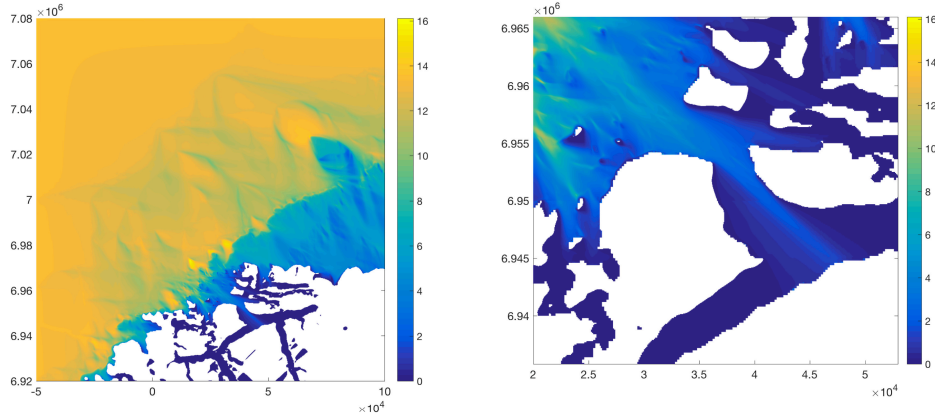
8

Figure 5: Significant wave height distribution of Sulafjord from swan simulation, to the left: the whole domain Hs distribution, to the right: Hs distribution at Sulasjord
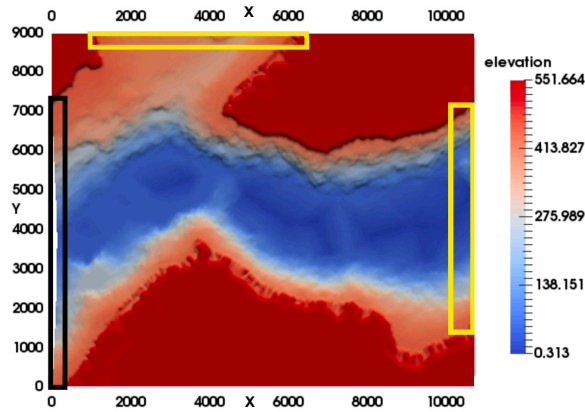

Figure 6: The bathymetry and numerical tank set up of Sulafjord CFD simulation

Table 2: The comparison of the wave properties at probes from the SWAN simulation, the regular wave CFD simulation and the irregular wave CFD simulation

Probes	SWAN		Regular wave CFD		Irregular wave CFD	
	H_s	T_m	H_m	T_m	H_s	T_m
D	4.67	9.95	5.33	16.86	6.91	8.38
A	2.57	9.71	7.31	16.92	5.11	7.53
B	2.28	9.37	7.41	16.97	5.12	8.68

4 CONCLUSIONS

The CFD simulation of the Sulafjord presents a good wave transformation process with reasonable computational resources. This gives confidence to large scale CFD simulations. As a
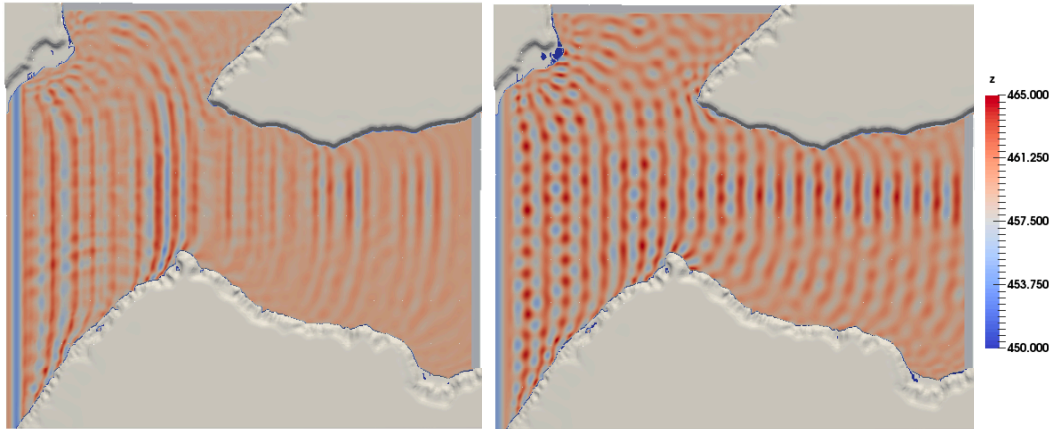
9

Figure 7: Wave pattern and free-surface of the regular wave CFD simulation at Sulafjord, to the left: irregular wave simulation; to the right regular wave simulation

first large scale CFD wave application on record for Norwegian fjords with deep water conditions, the detailed simulation results show the great potential of CFD capacity and introduce many promising topics for further development. The combination of SWAN and REEF3D reduces the cost on time and computational resources tremendously. The practice lays the foundation for the future development of an integrated numerical model consisting of CFD, Boussinesq model and fully non-linear potential flow model.

The uncertainties in the simulations and comparisons provoke the topic of developing a CFD simulation with a directional wave spectrum. Multi-chromatic waves and wave directional spreading functions are to be implemented in the future study. The field measurements for the duration of one whole year is needed to compare with the simulations. In conclusion, CFD models can be effectively applied on large scale wave simulation in Norwegian fjords and REEF3D shows satisfying capacity of carrying out such simulations. The attempt to optimise the advantages of each existing wave model and combine different models also shows promising potential.

Acknowledgement

References

Alagan Chella, M., Bihs, H., Myrhaug, D. and Muskulus, M. (2017). Breaking solitary waves and breaking wave forces on a vertically mounted slender cylinder over an impermeable

sloping seabed. *Journal of Ocean Engineering and Marine Energy*, **3**(1), 1–19. ISSN 2198-6452. doi:10.1007/s40722-016-0055-5.

Berthelsen, P.A. and Faltinsen, O.M. (2008). A local directional ghost cell approach for incompressible viscous flow problems with irregular boundaries. *Journal of Computational Physics*, **227**(9), 4354 – 4397. ISSN 0021-9991. doi: http://dx.doi.org/10.1016/j.jcp.2007.12.022.

Bihs, H. and Kamath, A. (2016). A combined level set/ghost cell immersed boundary representation for floating body simulations. *International Journal for Numerical Methods in Fluids*, n/a–n/a. ISSN 1097-0363. doi:10.1002/fld.4333. Fld.4333.

Bihs, H., Kamath, A., Chella, M.A., Aggarwal, A. and ivind A. Arntsen (2016). A new level set numerical wave tank with improved density interpolation for complex wave hydrodynamics. *Computers Fluids*, **140**, 191 – 208. ISSN 0045-7930. doi: http://dx.doi.org/10.1016/j.compfluid.2016.09.012.

Chi-Wang, S. and Stanley, O. (1988). Efficient implementation of essentially non-oscillatory shock-capturing schemes. *Journal of Computational Physics*, **77**(2), 439–471.

Ellevset, O. (2012). Project overview coastal highway route E39.

Falgout, R.D., Jones, J.E. and Yang, U.M. (2006). Conceptual interfaces in hypre. *Future Gener. Comput. Syst.*, **22**(1-2), 239–251. ISSN 0167-739X. doi:10.1016/j.future.2003.09.006.

Griebel, M., Dornseifer, T. and Neunhoeffer, T. (1998). *Numerical Simulation in Fluid Dynamics: A Practical Introduction.* Society for Industrial and Applied Mathematics, Philadelphia, PA, USA. ISBN 0-89871-398-6.

Guang-Shan, J. and Chi-Wang, S. (1996). Efficient implementation of weighted eno schemes. *Journal of Computational Physics*, **126**(1), 202–228.

Hasselø, J.A. (2015). Prosjektutviklingsmodell -teknologi. http://www.vegvesen.no/Euro paveg/E39sulafjorden/dokumenter.

HYPRE (2016). Hypre: Scalable linear solvers and multigrid methods. http://comput ation.llnl.gov/projects/hypre-scalable-linear-solvers-multigrid-methods.

Jacobsen, N., Fuhrman, D. and Fredse, J. (2012). A wave generation toolbox for the open-source cfd library: Openfoam. *International Journal for Numerical Methods in Fluids*, **70**(9), 1073–1088. ISSN 0271-2091. doi:10.1002/fld.2726.

Kamath, A., Chella, M.A., Bihs, H. and Arntsen, Ø.A. (2016). Breaking wave interaction with a vertical cylinder and the effect of breaker location. *Ocean Engineering*, **128**, 105 – 115. ISSN 0029-8018. doi:http://dx.doi.org/10.1016/j.oceaneng.2016.10.025.

Madsen, P.A. and Srensen, O.R. (1992). A new form of the boussinesq equations with improved linear dispersion characteristics. part 2. a slowly-varying bathymetry. *Coastal Engineering*, **18**(3), 183 – 204. ISSN 0378-3839. doi:http://dx.doi.org/10.1016/0378-3839(92)90019-Q.

Mayer, S., Garapon, A. and Srensen, L.S. (1998). A fractional step method for unsteady free-surface flow with applications to non-linear wave dynamics. *International Journal for Numerical Methods in Fluids*, **28**(2), 293–315. ISSN 1097-0363. doi:10.1002/(SICI)1097-0363(19980815)28:2¡293::AID-FLD719¿3.0.CO;2-1.

Norgeskart (2017). Sulafjord. http://www.norgeskart.no/?ga= 1.148519543.1531380854. 14846589939/26136/6963625/ -land/+sjo.

NORSOK (2007). Actions and action effect. Standard N-003, Norwegian Oil Industry Association and the Federation of Norwegian Industry, Strandveien 18, Lysaker, Norway.

Osher, S. and Sethian, J.A. (1988). Fronts propagating with curvature-dependent speed: Algorithms based on hamilton-jacobi formulations. *Journal of Computational Physics*, **79**(1), 12 – 49. ISSN 0021-9991. doi:http://dx.doi.org/10.1016/0021-9991(88)90002-2.

Shepard, D. (1968). A two-dimensional interpolation function for irregularly-spaced data. In: *Proceedings of the 1968 23rd ACM National Conference*, ACM '68, 517–524. ACM, New York, NY, USA. doi:10.1145/800186.810616.

Statensvegvesen (2015). Illustrasjonskart E39 sulafjorden. http://www.vegvesen.no/Euro paveg/e39sulafjorden.

SWAN (2006). *SWAN User Manual*. Delft University of Technology, 2600 GA Delft, the Netherlands.

Thomas, T.J. and Dwarakish, G. (2015). Numerical wave modelling a review. *Aquatic Procedia*, **4**, 443 – 448. ISSN 2214-241X. doi:http://dx.doi.org/10.1016/j.aqpro.2015.02.059.

Van Der Vorst (1992). Bi-cgstab: A fast and smoothly converging variant of bi-cg for the solution of nonsymmetric linear systems. *SIAM Journal on Scientific and Statistical Computing*, **13**(2), 631–644.